AIP | Journal of Applied Physics

Topological states ruled by stacking faults in Bi2Se3 and Bi2Te3

L. Seixas, L. B. Abdalla, T. M. Schmidt, A. Fazzio, and R. H. Miwa

Citation: J. Appl. Phys. **113**, 023705 (2013); doi: 10.1063/1.4773325
View online: http://dx.doi.org/10.1063/1.4773325
View Table of Contents: http://jap.aip.org/resource/1/JAPIAU/v113/i2
Published by the American Institute of Physics.

Related Articles

Spatially resolved study of quantum efficiency droop in InGaN light-emitting diodes
Appl. Phys. Lett. 101, 252103 (2012)

On the origin of basal stacking faults in nonpolar wurtzite films epitaxially grown on sapphire substrates
J. Appl. Phys. 112, 113518 (2012)

The structure of dislocations in (In,Al,Ga)N wurtzite films grown epitaxially on (0001) or (112) GaN or AlN substrates
J. Appl. Phys. 112, 113507 (2012)

Applied stress controls the production of nano-twins in coarse-grained metals
Appl. Phys. Lett. 101, 231903 (2012)

On the role of stacking faults on dislocation generation and dislocation cluster formation in multicrystalline silicon
J. Appl. Phys. 112, 103528 (2012)

Additional information on J. Appl. Phys.

Journal Homepage: http://jap.aip.org/
Journal Information: http://jap.aip.org/about/about_the_journal
Top downloads: http://jap.aip.org/features/most_downloaded
Information for Authors: http://jap.aip.org/authors

ADVERTISEMENT

Downloaded 21 Feb 2013 to 128.113.122.179. Redistribution subject to AIP license or copyright; see http://jap.aip.org/about/rights_and_permissions

JOURNAL OF APPLIED PHYSICS 113, 023705 (2013)

Topological states ruled by stacking faults in Bi_2Se_3 and Bi_2Te_3

L. Seixas,[1] L. B. Abdalla,[1] T. M. Schmidt,[2] A. Fazzio,[1] and R. H. Miwa[2]
[1]*Instituto de Física, Universidade de São Paulo, C. P. 66318, 05315-970 São Paulo, SP, Brazil*
[2]*Instituto de Física, Universidade Federal de Uberlândia, C. P. 593, 38400-902 Uberlândia, MG, Brazil*

(Received 20 October 2012; accepted 10 December 2012; published online 9 January 2013)

Extended defects like stacking faults (SFs) can originate topologically protected metallic states in bulk topological insulators (TIs). These induced topological states are a response to the weakening of the inter-layer van der Waals interactions due to the SF defect. In TI thin films, the degeneracy of Dirac bands of opposite surfaces can be lifted upon the formation of SF defects. Such slab asymmetry can promote a net spin current, in the absence of backscattering processes, in thin film made of TIs. These results have been obtained by fully relativistic first principles calculations. © *2013 American Institute of Physics*. [http://dx.doi.org/10.1063/1.4773325]

I. INTRODUCTION

Three dimensional topological insulators (TIs), like Bi_2Se_3 and Bi_2Te_3, exhibit energy gaps in the bulk phase, while on the surfaces, they present metallic surface states (SSs). A parity inversion on the (bulk) conduction and valence bands, ruled by spin-orbit coupling, promotes the formation of topologically protected metallic SSs, with linear energy band dispersion, giving rise to the so called Dirac-points.[1,2] The Dirac-cone SSs are characterized by a chiral spin-texture protected by time-reversal symmetry, and thus backscattering processes by time-reversal invariant impurities or defects are forbidden.[2] The formation of intrinsic spin-polarized current has been the strongest appeal for technological applications of TIs, especially in spintronics. However, electronic scattering channels have been observed in TIs due to the presence of continuous bulk states near the Dirac-point.[3,4]

Structural parameters of TIs play an important role on the electronic properties of those protected (metallic) SSs. For instance, (i) the formation of an energy gap in thin films, below six (three) quintuple layers (QLs) of Bi_2Se_3 (Bi_2Te_3), due to the interaction between the SSs of opposite edges[5,6] and (ii) the tuning process of the topological phase through mechanical strain or alloy concentration, like in $TlBiSe_2$ and $Bi_{2-x}Ca_xSe_3$.[3,7–9] It is worth to note that in thin free standing symmetric films of TIs, there is no finite net spin current, since the (topologically protected) SSs of opposite edges are degenerated and present opposite helicities.[10,11] There are several ways to break such inversion symmetry, namely by application of external field,[10] interaction with a solid substrate,[5] and adsorption of magnetic ions in one side of the TI thin film.[11,12] In those asymmetric TI slabs, we may find a net spin polarized current along a given direction parallel to the TI surface, mostly localized on the topmost surface atoms.

Each QL of Bi_2Se_3 (Bi_2Te_3) is composed by two atoms of Bi and three atoms of Se (Te), attached by Bi–Se (Bi–Te) chemical bonds, while the QL–QL interaction is weak, mainly ruled by van der Waals (vdW) type interaction. Indeed, recent studies indicate the formation of extended defects like stacking-faults (SFs) and energetically stable twin structures, along the [0001] direction of Bi_2Se_3 and Bi_2Te_3 films.[13,14] Based upon the scenario described above, we believe that it is worth to investigate, through *ab initio* atomistic simulations, the role played by such extended defects on the structural and electronic properties of TIs.

In this work, we show that extended defects like SFs promote the formation of topologically protected metallic bands embedded within the QLs of bulk TIs. Meanwhile, thin films of TIs become asymmetric due to the presence of SFs, giving rise to an energy splitting of the Dirac-points. Upon the presence of SFs near the TI surface, the binding energy of the Dirac-point is reduced, lying above the continuous bulk states. Those findings allow us to infer that we may have a finite net spin current, in the absence of electronic back scattering channels, in thin films of TIs ruled by the presence of SFs.

II. METHODOLOGY

We performed *ab initio* investigation, using the density functional theory (DFT),[15,16] of SFs in Bi_2Se_3 and Bi_2Te_3 TIs. For the exchange and correlation potential, we have considered the local density approximation (LDA)[17] for the calculation of the QL–QL binding energies, while the electronic band structure properties were calculated by using the generalized gradient approximation (GGA).[18] The spin-orbit interactions were self-consistently treated by using the fully relativistic pseudopotential within the projector augmented wave (PAW) method.[19] We used the Vienna *ab initio* simulation package (VASP).[20] A plane-wave basis set was used, with a cut-off energy of 212 eV. The Brillouin zone was sampled, according to the Monkhorst-Pack scheme,[21] by using a number of *k*-points (mesh of $5 \times 5 \times 1$) such that the total energy was converged. The (111) surface of Bi_2Se_3 and Bi_2Te_3 was investigated using the slab method with a vacuum layer of at least 20 Å. Here, we have used a thickness up to 10 QLs, keeping the experimental lattice parameter.

III. RESULTS

The bulk phase of Bi_2Se_3 and Bi_2Te_3 presents a rhombohedral structure composed by QLs piled up along the *c* axis of a hexagonal crystal lattice, [0001] direction. A set of three QLs, sublattices A, B, and C in Fig. 1, represents the periodic unit of Bi_2Se_3 or Bi_2Te_3. The five atoms of a QL are attached through covalent bonds, while the interaction

 © 2013 American Institute of Physics

Downloaded 21 Feb 2013 to 128.113.122.179. Redistribution subject to AIP license or copyright; see http://jap.aip.org/about/rights_and_permissions

between adjacent QLs is mostly ruled by vdW interactions.[22] In this case, we can infer that the formation of SFs and twin structures along the c axis, between QLs in Bi_2Se_3 and Bi_2Te_3, is quite likely processes.

The stacking configuration for the perfect system is ABCABCABC, where each QL is rotated by 120° with respect to the next one, Fig. 1(b). We have considered the formation of SFs by (i) removing a QL, e.g., ABABCABC or (ii) by adding an extra QL layer, e.g., ABBCABCABC, as depicted in Figs. 1(c) and 1(d), respectively. In (i) we have the so called intrinsic SF (ISF), and in (ii) we have an extrinsic SF (ESF).[23] For each SF configuration, the equilibrium distance between the QLs was obtained by minimizing the total energy as a function of the vertical distance (Δz) between two QLs.[24] Our results of Δz are shown in Fig. 2. We find that, indeed, the perfect stacking (AB, BC, or CA) represents the energetically most favorable configuration, with a vertical equilibrium distance of 2.15 Å (Bi_2Se_3) and 2.56 Å (Bi_2Te_3), both in good agreement with experimental results[25] and *ab initio* calculations.[22,26] The vertical equilibrium distances and the total energies increase upon the presence of SFs, and thus indicating that the formation of SFs is endothermic. For the ESF in Bi_2Se_3 and Bi_2Te_3, we find a total energy increase (ΔE) of 107 and 82 mJ/m^2, respectively. At the equilibrium geometry, we obtain Δz of 2.40 Å (ESF in Bi_2Se_3) and 2.91 Å (ESF in Bi_2Te_3), that is, an increase of the interlayer spacing of 12% and 15%, respectively. Meanwhile for ISF in Bi_2Se_3 and Bi_2Te_3, we find Δz of 3.15 and 3.76 Å, respectively, and a ΔE increasing by 212 mJ/m^2 (ISF in Bi_2Se_3) and 196 mJ/m^2 (ISF in Bi_2Te_3). It is worth to note that at the AC, CB, or CA ISF interfaces, the Se or Te atoms are perfectly aligned along the c axis, weakening the QL–QL interaction and increasing the vertical equilibrium distance up to 47%. Further total energy comparison shows that the sequence of the energetic stability pristine → ESF → ISF is ruled by the ion-ion electrostatic interaction at the interface between the faulted QLs. Our findings for SF formation energies are comparable to the ones obtained for other materials like, Si 33 (ISF) and 26 (ESF) mJ/m^2,[23] Ni 187 (ISF) 149 (ESF), and Rh 750 (ISF) and 291 (ESF) mJ/m^2.

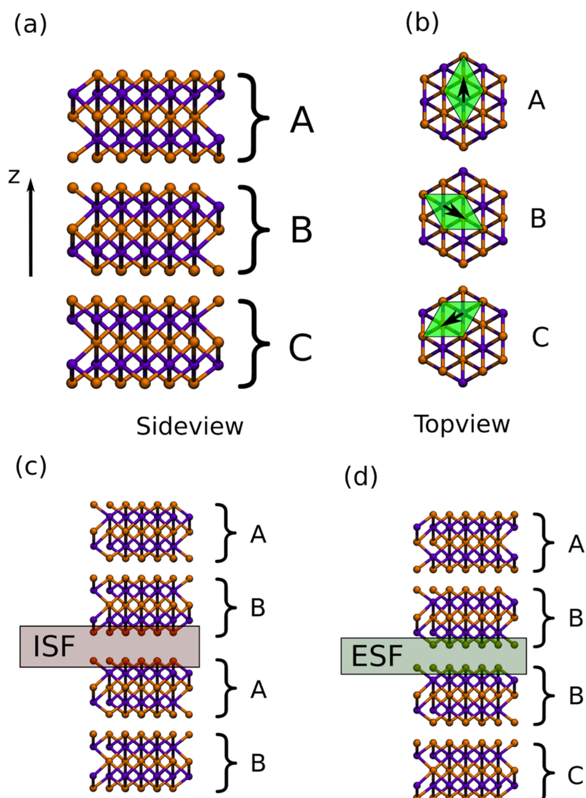

FIG. 1. Structural representation of Bi_2Se_3 and Bi_2Te_3. (a) Side view of three inequivalent QLs stacking along the z-axis, [0001] direction. (b) Top view of each QL: A, B, and C, respectively. The green cells and black arrows represent the relative orientation among QLs. Structural models of SFs, (c) intrinsic stacking fault, and (d) extrinsic stacking fault.

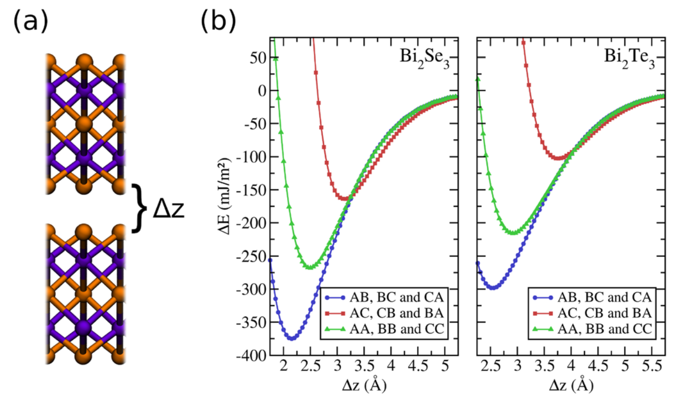

FIG. 2. (a) Representation of the separation between QLs, Δz. (b) Binding energies between QLs, as a function of Δz, for ISF and ESF in Bi_2Se_3 (left) and Bi_2Te_3 (right).

The formation of SFs gives rise to electronic states lying within the band-gap of the pristine bulk phase. Figure 3 presents the electronic band structure for wave vectors parallel to the SF plane ($\Gamma-K$ and $\Gamma-M$ directions). Shaded regions indicate the projected band structure of pristine Bi_2Se_3 and Bi_2Te_3 systems. For ESF in Bi_2Se_3, we find an occupied state slightly above the valence band maximum (VBM) at the Γ point of pristine Bi_2Se_3, $v1$ in Fig. 3(b). Here, similar to SFs in silicon,[23] $v1$ follows the energy dispersion of the (pristine) bulk system. Meanwhile, for ESF in Bi_2Te_3, we find a parabolic SF band lying within the band-gap [$c1$ in Fig. 3(d)]. Here, different from Bi_2Se_3, the SF state does not follow the energy dispersion of the Bi_2Te_3 (pristine) bulk phase. The presence of SF states, within the band-gap, has been strengthened upon the formation of ISFs. For ISF in Bi_2Se_3, the occupied SF state $v1$ no longer follows the energy dispersion of the (pristine) bulk phase, Fig. 3(a). In this case, along the $\Gamma-K$ direction, $v1$ moves upward within the band-gap, while along the $\Gamma-M$ direction, it remains resonant within the valence band of Bi_2Se_3. In addition, we find an empty (parabolic) state, $c1$ in Fig. 3(a), slightly below the conduction band minimum at the Γ point. In strike contrast, we find topologically protected metallic bands for ISF in Bi_2Te_3, $c1$, and $c2$ in Fig. 3(c). Those metallic states are localized on the Te atoms at the SF interface.

The formation of electronic states within the band-gap of TIs, by increasing the QL–QL distance, Δz, is quite an expected process. That is, the increase of Δz promotes the formation of surface-like environment at the (expanded) interface region, giving rise to a topological/trivial (e.g.,

Downloaded 21 Feb 2013 to 128.113.122.179. Redistribution subject to AIP license or copyright; see http://jap.aip.org/about/rights_and_permissions

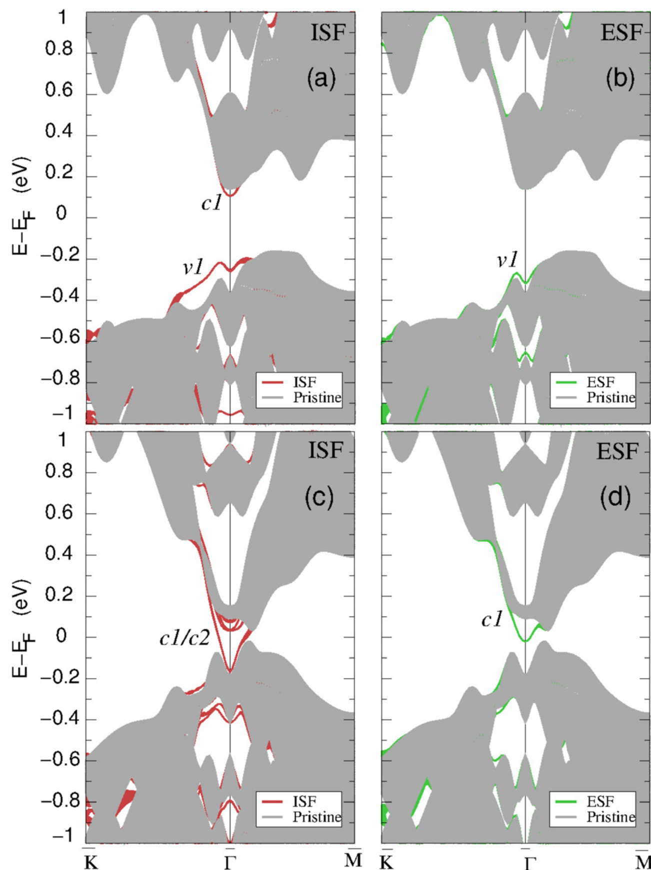

FIG. 3. Electronic band structure of Bi_2Se_3 bulk phase with an ISF (a) and ESF (b). (c) and (d) The ISF and ESF Bi_2Te_3 bulk phase. Shaded regions indicate the bulk projected band structure.

Bi_2Se_3/vacuum) interface. In order to verify such statement, we examined the evolution of the electronic states as a function of the "vacuum-size" between two consecutive QLs. Our results, depicted in Fig. 4, reveal the formation of partially occupied states for $\Delta z = 5.15$ Å in Bi_2Se_3, while the Dirac-point occurs at $\Delta z = 6.15$ Å. For Bi_2Te_3, we find smaller values of Δz to obtain metallic bands (3.36 Å) and the Dirac-point (3.56 Å). These latter results are in accordance with the formation of topologically protected metallic states due to the formation of ISF in Bi_2Te_3 ($\Delta z = 3.76$ Å), as shown in Fig. 3(c). The smaller Δz in Bi_2Te_3, to obtain the protected metallic states, can be attributed to the smaller forbidden energy gap in Bi_2Te_3, which favor the connection between the topologically inverted bands and the trivial insulator bands at the Bi_2Te_3/vacuum interface.

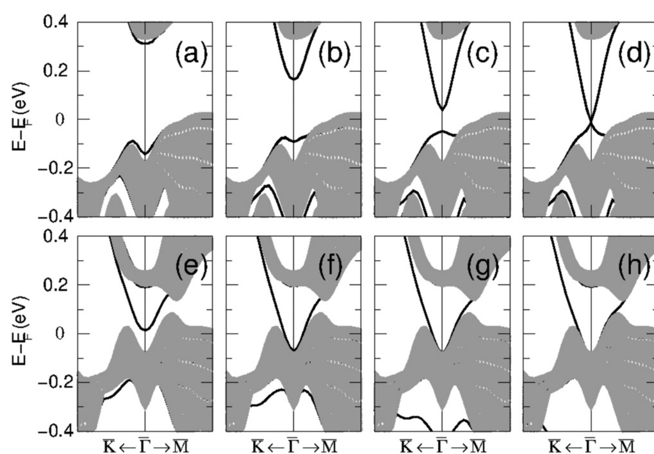

FIG. 4. Evolution of the electronic states of Bi_2Se_3 as function of the QL–QL distance, Δz: (a) 2.50 Å, (b) 3.15 Å, (c) 4.15 Å, (d) 7.15 Å; and for Bi_2Te_3: (e) 2.91 Å, (f) 3.26 Å, (g) 3.76 Å, (h) 7.56 Å.

In accordance with previous theoretical studies,[10] the Dirac-point lies below the projected VBM, 0.06 eV (Bi_2Se_3) and 0.12 eV (Bi_2Te_3). Such energy position of the Dirac-point promotes the electronic scattering between the (metallic) SSs near the Fermi level and the (continuous) projected bulk states.[4] We find that the presence of SFs buried in the bulk region, i.e., far from the surface region, weakly perturbs the SSs of Bi_2Se_3 and Bi_2Te_3. The energy position and dispersion have been maintained as the ones of pristine systems. On the other hand, for SFs nearby the surface layers, we face a different scenario. For the Bi_2Se_3 surface, an ESF gives rise to a slightly upward displacement, by ~50 meV [Fig. 5(a)], of the Dirac-point when compared with the one of the pristine system. For the ISF, such upward (energy) displacement is ~94 meV [Fig. 5(b)]. Similar energy splitting at the Dirac-point has been verified for thin films of Bi_2Se_3 by the application of an external electric field.[10] For both SFs, we find that the Dirac-point lies above the bulk projected VBM of Bi_2Se_3. Here, we can infer that the presence of SF nearby the topmost QLs may suppress the scattering channels between the metallic SSs near the Dirac point and the continuous bulk states for Bi_2Se_3. However, different from the Bi_2Se_3 surface, the formation of SFs in Bi_2Te_3 weakly perturbs the energy position of the Dirac-point. Thus, scattering channels between the metallic surface states and the continuous bulk states will be maintained, even upon the presence of SFs in Bi_2Te_3 surfaces.

There is no net spin-polarized current in symmetric thin films of TIs, since the metallic SSs of opposite edges are degenerated and present opposite helicities. On the other hand, as depicted in Fig. 5, such energy degeneracy can be removed upon the presence of SFs nearby the topmost

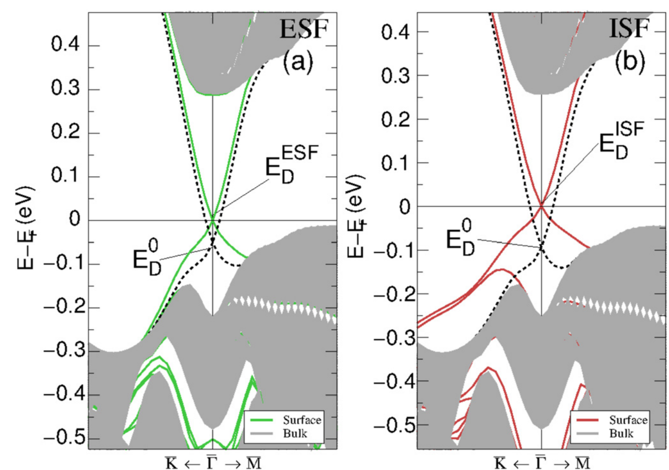

FIG. 5. Electronic band structure of Bi_2Se_3 at the presence of (a) ESF, and (b) ISF in thin films of Bi_2Se_3. Solid lines represent the electronic band structure of the Bi_2Se_3 (0001) surface at the presence of stacking faults, dashed lines indicate the electronic band structure of the pristine system, and the shaded regions represent the projected Bi_2Se_3 bulk band structure. E_D^{ESF} (E_D^{ISF}) indicates the energy position of the Dirac point at the presence of ESF (ISF), and E_D^0 indicates the energy position of the Dirac point for the pristine system.

Downloaded 21 Feb 2013 to 128.113.122.179. Redistribution subject to AIP license or copyright; see http://jap.aip.org/about/rights_and_permissions

surface layers. The formation of ESF in Bi_2Se_3 surface promotes an upward displacement, by 50 meV, of the Dirac-point [solid lines in Fig. 5(a)] when compared with the one of the pristine Bi_2Se_3 surface, that is, $E_D^{ESF} - E_D^0 = 50$ meV. Meanwhile for the ISF, we find $E_D^{ISF} - E_D^0 = 94$ meV as shown in Fig. 5(b). Those results allow us to predict a finite net spin-polarized current, composed by holes (electrons) on the edge with (without) SFs, by considering electronic chemical potential (μ_e) within the following energy window, $E_D^0 < \mu_e < E_D^{ESF}$ or $E_D^0 < \mu_e < E_D^{ISF}$. That is, addressing the development of spintronic devices, we find that spin-polarized current can be obtained by tuning, in a suitable way, the position of the electronic chemical potential near the Dirac point in thin films of TIs upon the presence of SFs.

IV. SUMMARY

In summary, based on *ab initio* total energy calculations, we examined the electronic and structural properties of stacking faults in Bi_2Se_3 and Bi_2Te_3 TIs. We find the formation of topologically protected states embedded at the faulted interface of Bi_2Te_3 bulk system. Meanwhile, the insulating character has been preserved in Bi_2Se_3 bulk upon the presence of stacking faults. For stacking faults nearby the surface layers of Bi_2Se_3, we find that the Dirac-point moves upward with respect to the one of the pristine system, lying above the continuous bulk states. In this case, there is a suppression of the scattering channels between the topologically protected metallic surface states and the continuous Bi_2Se_3 bulk states. By considering thin films of Bi_2Se_3, it becomes asymmetric upon the presence of stacking faults near one surface edge. Such asymmetry promotes a net spin current on the TI surface, for the electronic states near the Dirac-point. Those results open a door for potential applications of TIs in spintronic devices.

ACKNOWLEDGMENTS

The authors acknowledge financial support from the Brazilian agencies CNPq/INCT, CAPES, FAPEMIG, and FAPESP, and the computational support from CENAPAD/SP.

[1]H. Zhang, C. Liu, X. Qi, X. Dai, Z. Fang, and S. Zhang, Nat. Phys. **5**, 438 (2009).
[2]M. Z. Hasan and C. L. Kane, Rev. Mod. Phys. **82**, 3045 (2010).
[3]K. Kuroda, M. Ye, A. Kimura, S. V. Eremeev, E. V. Krasovskii, E. V. Chulkov, Y. Ueda, K. Miyamoto, T. Okuda, K. Shimada *et al.*, Phys. Rev. Lett. **105**, 146801 (2010).
[4]S. Kim, M. Ye, K. Kuroda, Y. Yamada, E. E. Krasovski, E. V. Chulkov, K. Miyamoto, M. Nakatake, T. Okuda, Y. Ueda *et al.*, Phys. Rev. Lett. **107**, 056803 (2011).
[5]Y. Zhang, K. He, C. Chang, C. Song, L. Wang, X. Chen, J. Jia, Z. Fang, X. Dai, W. Shan *et al.*, Nat. Phys. **6**, 584 (2010).
[6]K. Park, J. J. Heremans, V. W. Scarola, and D. Minic, Phys. Rev. Lett. **105**, 186801 (2010).
[7]S. M. Young, S. Chowdhury, E. J. Walter, E. J. Mele, C. L. Kane, and A. Rappe, Phys. Rev. B **84**, 085106 (2011).
[8]D. Hsieh, Y. Xia, D. Qian, L. Wray, J. H. Jill, J. Osterwalder, L. Patthey, J. G. Checkelsky, N. P. Ong, A. V. Fedorov *et al.*, Nature **460**, 1101 (2009).
[9]S. Xu, Y. Xia, L. A. Wray, S. Jia, F. Meier, J. H. Dill, J. Osterwalder, B. Stomski, A. Bansil, H. Lin *et al.*, Science **332**, 560 (2011).
[10]O. V. Yazyev, J. E. Moore, and S. G. Louie, Phys. Rev. Lett. **105**, 266806 (2010).
[11]H. Jin, J. Song, and A. J. Freeman, Phys. Rev. B **83**, 125319 (2011).
[12]T. M. Schmidt, R. H. Miwa, and A. Fazzio, Phys. Rev. B **84**, 245418 (2011).
[13]B. Jariwala and D. V. Shah, J. Cryst. Growth **318**, 1179 (2011).
[14]D. L. Medlin, Q. M. Ramasse, C. D. Spataru, and N. Y. C. Yang, J. Appl. Phys. **108**, 043517 (2010).
[15]P. Hohenberg and W. Kohn, Phys. Rev. **136**, B864 (1964).
[16]W. Kohn and L. J. Sham, Phys. Rev. **140**, A1133 (1965).
[17]D. M. Ceperley and B. J. Alder, Phys. Rev. Lett. **45**, 566 (1980).
[18]J. P. Perdew, K. Burke, and M. Ernzerhof, Phys. Rev. Lett. **77**, 3865 (1996).
[19]P. E. Blüchl, Phys. Rev. B **50**, 17953 (1994).
[20]G. Kresse and J. Furthmüller, Phys. Rev. B **54**, 11169 (1996).
[21]H. J. Monkhorst and J. D. Pack, Phys. Rev. B **13**, 5188 (1976).
[22]W. Zhang, R. Yu, H. Zhang, X. Dai, and Z. Fang, New J. Phys. **12**, 065013 (2010).
[23]M. Y. Chou, M. L. Cohen, and S. G. Louie, Phys. Rev. B **32**, 7979 (1985).
[24]The calculations were performed by considering the total energy as a function of the distance between two isolated QLs. The atomic positions were not allowed to relax.
[25]H. Lind and S. Lindin, Solid State Sci. **5**, 47 (2003).
[26]H. Lind, S. Lindin, and U. Häussermann, Phys. Rev. B **72**, 184101 (2005).

Downloaded 21 Feb 2013 to 128.113.122.179. Redistribution subject to AIP license or copyright; see http://jap.aip.org/about/rights_and_permissions